

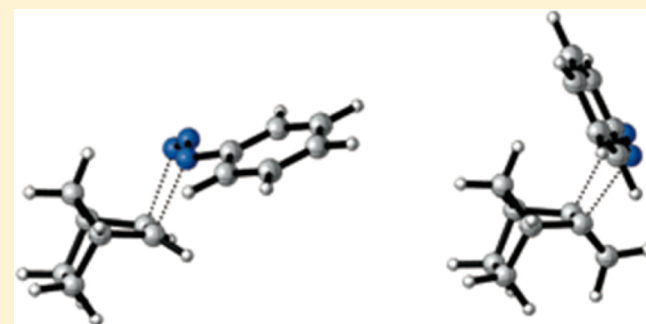
# Alkene Distortion Energies and Torsional Effects Control Reactivities, and Stereoselectivities of Azide Cycloadditions to Norbornene and Substituted Norbornenes

Steven A. Lopez and K. N. Houk\*

Department of Chemistry and Biochemistry, University of California, Los Angeles, California 90095-1569, United States

## Supporting Information

**ABSTRACT:** The transition structures for 1,3-dipolar cycloadditions of phenyl azide to norbornene derivatives were located with quantum mechanical methods. Calculations were carried out with M06-2X/6-311G(d,p) and SCS-MP2/6-311G(d,p)//M06-2X/6-311G(d,p) methods. The calculated activation barriers strongly correlate with transition state distortion energies ( $\Delta E_d^\ddagger$ ) but not with the reaction energies. Strain-promoted reactions are accelerated because it is easy to distort the strained reactants to a pyramidalized transition state geometry; a correlation of cycloaddition rates with substrate distortion was found for the bicyclic and tricyclic alkenes studied here. The stereoselectivities of reactions of norbornene derivatives are controlled primarily by torsional effects that also



influence alkene pyramidalization. These reactions are distortion-

accelerated.

## INTRODUCTION

The unusual reactivity and high exo stereoselectivity of norbornene in cycloadditions has long been of great mechanistic interest<sup>1</sup> and has recently led to useful bioorthogonal chemistry involving norbornenes.<sup>2,3</sup> Huisgen and co-workers first observed the unexpectedly high reactivity of norbornene and its derivatives along with a great preference for exo cycloadditions of phenyl azide and other 1,3-dipoles; other groups have confirmed these observations.<sup>4–7</sup> After accounting for factors such as strain by calculating hydrogenation energies using MM2 computations, Huisgen found that the exo activation barriers are 1–3 kcal/mol lower than expected. He attributed this reduced activation energy to “factor X”.<sup>8</sup> Our group discovered that “factor X” is due to exceptionally favorable torsional effects in the exo transition state.<sup>9</sup>

We have now investigated the transition states for 1,3-dipolar cycloadditions of strained, pyramidalized alkenes with phenyl azide, an ambiphilic 1,3-dipole, and a common substrate in Sharpless' Click chemistry.<sup>10</sup> We report computed transition structures and activation barriers for cycloadditions to a number of norbornenes and to the simple alkenes, *cis*-2-butene (1) and cyclohexene (2). In addition to norbornene, tricyclic hydrocarbons with norbornene fused to cyclopropene or cyclobutene (4 and 5), *syn*-sesquinorbornene (6), and *anti*-sesquinorbornene (7) were studied. These compounds are shown in Figure 1. The unstrained planar alkenes (1, 2) are used as a standard to which the reactivity of pyramidalized alkenes (3–6) can be compared.

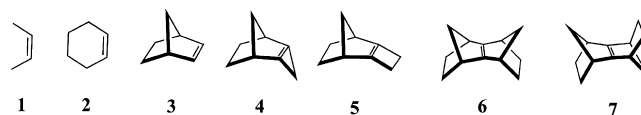


Figure 1. Series of dipolarophiles studied.

## COMPUTATIONAL METHODS

All computations were carried out with the Gaussian 09<sup>11</sup> series of programs. The stationary points were located using M06-2X/6-311G(d,p),<sup>12</sup> and frequency calculations on these stationary points provide activation enthalpies and free energies. Vibrational analysis confirmed all stationary points to be first-order saddle points or minima with no imaginary frequencies. The ab initio method MP2 included the spin-component-scaled (SCS) correction, which uses standard parameters with the application of frozen-core approximation for nonvalence-shell electrons. SCS-MP2/6-311G(d,p)<sup>13</sup> single points used the M06-2X/6-311G(d,p)-optimized geometries to give independent estimates of barrier heights and reaction energies. (Energies given in the Supporting Information.) Solvation corrections were computed on gas-phase geometries with M06-2X/6-311G(d,p). On the basis of the results of a study performed by our group,<sup>14</sup> the corrections used the CPCM model<sup>15</sup> using UAKS radii for two solvents (CCl<sub>4</sub> and Et<sub>2</sub>O) and more accurately reproduce experimental conditions. A quasiharmonic correction was applied during the entropy calculation by setting all frequencies that are less than 100

Special Issue: Howard Zimmerman Memorial Issue

Received: June 18, 2012

Published: July 5, 2012

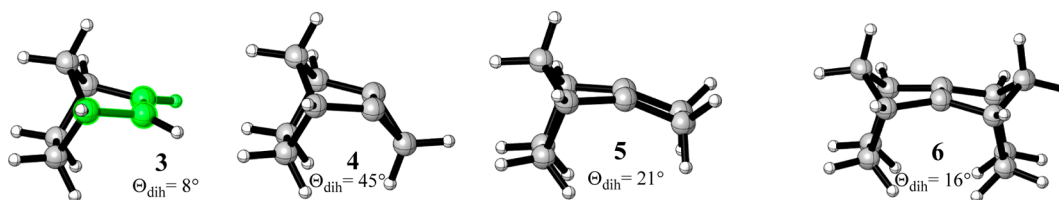


Figure 2. Optimized minima of 3–6 as calculated by M06-2X/6-311G(d,p). The green atoms in 3 define  $\theta_{\text{dih}}$ .

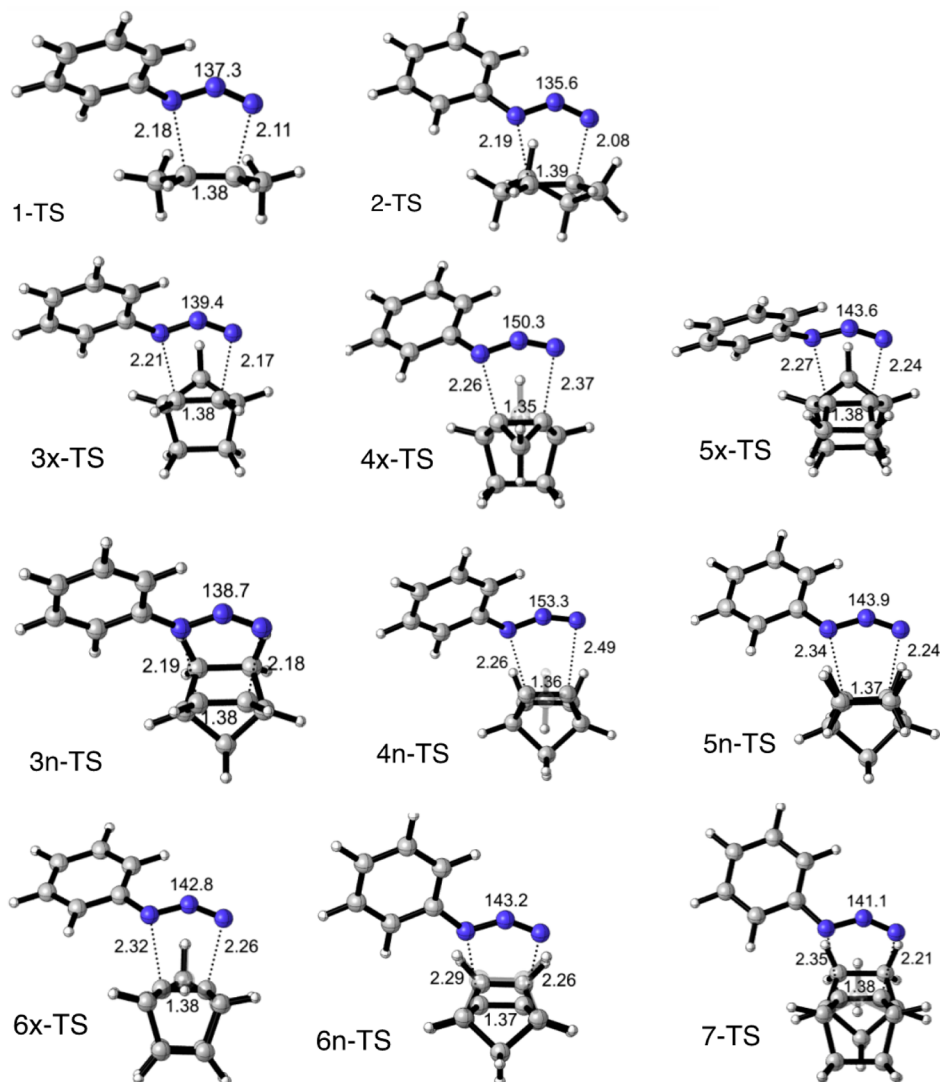


Figure 3. Optimized transition structures of the 1,3-dipolar cycloaddition of phenyl azide to alkenes 1–7 as calculated by M06-2X/6-311G(d,p). Bond lengths are reported in Å.

$\text{cm}^{-1}$  to  $100 \text{ cm}^{-1}$ .<sup>16,17</sup> Both SCS-MP2 and M06-2X predict 2–5 kcal/mol higher barriers than experiment, likely due to overestimation of  $-T\Delta S^\ddagger$  for these bimolecular reactions in solution. A benchmarking study on the 1,3-dipolar cycloaddition of 48 different dipoles to ethylene and acetylene was done by our group.<sup>18</sup> G3B3 was adopted as the standard method for predicting activation barriers, and M06-2X and SCS-MP2//B3LYP were found to predict activation barriers closest to those from G3B3.<sup>18</sup>

## RESULTS/DISCUSSION

**Pyramidalization of Norbornenes.** Previous studies have shown that ring strain and ground-state angle distortion contribute greatly to the extent of alkene pyramidalization.<sup>19–21</sup>

Second-order Jahn–Teller distortion leads to stabilization resulting from mixing of  $2s$  orbitals of the alkene carbons with  $p$  orbitals which form the  $\pi$  bond.<sup>22</sup> Pyramidalization occurs in the endo direction for norbornene derivatives to minimize torsional strain.<sup>20</sup> The optimized structures of alkenes 3–6 are shown in Figure 2. The ideal bond angle for  $\text{sp}^2$ -hybridized carbons is  $120^\circ$ , while  $\text{sp}^3$  carbons have an ideal bond angle of  $109.5^\circ$ ; consequently, the smaller C–C=C angles in strained alkenes reduce the force constants for out-of-plane bending. We use  $\theta_{\text{dih}}$  to quantify the degree of pyramidalization in these alkenes. The torsional angle,  $\theta$ , designated by the green atoms of 3 in Figure 3 is subtracted from  $180^\circ$  to obtain the out-of-plane bending angle,  $\theta_{\text{dih}}$ .  $\theta_{\text{dih}} = 0^\circ$  when  $\theta = 180^\circ$ . This value is

identical to the “butterfly angle” ( $\psi$ ), as described by Williams.<sup>23</sup>  $\theta_{\text{dih}}$  is  $60^\circ$  for a perfectly  $\text{sp}^3$ -pyramidalized alkene. Our high-level DFT calculations compare well with previous results by Vazquez,<sup>24</sup> Williams,<sup>20</sup> and our group.<sup>9</sup> We report  $\theta_{\text{dih}}$  of  $8^\circ$ ,  $45^\circ$ ,  $21^\circ$ ,  $16^\circ$ , and  $0^\circ$  for alkenes 3, 4, 5, 6, and 7; they report  $7^\circ$ ,  $44^\circ$ ,  $18^\circ$ ,  $16^\circ$ , and  $0^\circ$  for the same alkenes.

**Transition Structures.** The optimized transition structures of the reactions of dipolarophiles (1–7) with phenyl azide are shown in Figure 3. The reactions are concerted, but the transition structures show that bond formation is slightly asynchronous. The dipolarophiles in the transition states all have nearly identical alkene bond lengths (1.35–1.39 Å). However, the  $\angle\text{NNN}$  and forming bond distances between the dipole and dipolarophile vary significantly through the series,  $136$ – $153^\circ$  and  $2.08$ – $2.49$  Å, respectively. The partial bond to the more electrophilic (unsubstituted) terminus of phenyl azide is somewhat shorter than the partial bond to the more nucleophilic terminus.

The transition structures for the planar alkenes *cis*-2-butene (1) and cyclohexene (2) are very similar, with  $\angle\text{NNN}$  of  $137^\circ$  and  $136^\circ$ , respectively. Both have average forming C–N bond lengths of 2.14 Å. *anti*-Sesquinorbornene is planar and has an earlier transition state, the result of increased steric clashes in the transition structure between the ethylene bridges of *syn*-sesquinorbornene. The exo transition structures for the norbornenes 3–6 have NNN angles that increase with increasing  $\theta_{\text{dih}}$  in the reactants; this correlates with the lower activation barriers and earlier transition states as  $\theta_{\text{dih}}$  increases. The exo transition structures for the reactions of 3, 5, and 4 with phenyl azide have  $\angle\text{NNN} = 139^\circ$ ,  $144^\circ$ , and  $150^\circ$ , respectively, and correspond to increasingly early transition states.

**Stereoselectivities.** The exo stereoselectivity seen in these reactions results from different torsional effects in exo and endo transition states. Figure 4 shows Newman projections along the 1,2 and 3,4 bonds in the 1,3-dipolar cycloaddition transition states of norbornene and phenyl azide. These torsional effects are representative of all of the pyramidalized alkenes discussed here. A nearly perfect staggered conformation about the C-1, C-2 bond can be seen for the exo transition structure (3x-TS) on

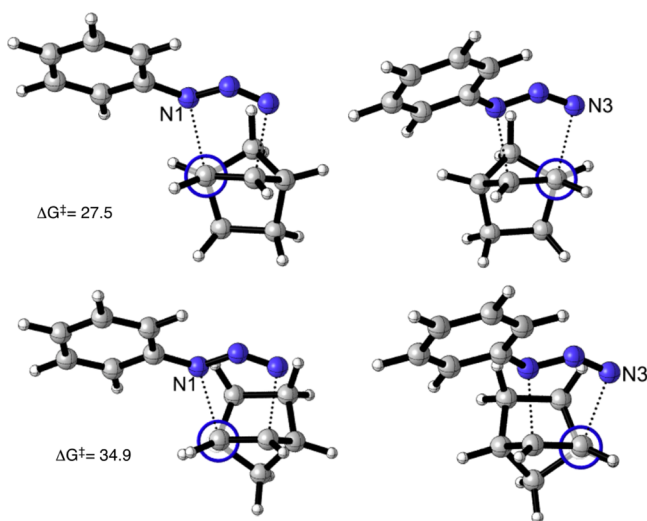


**Figure 4.** Newman projections for the cycloadditions of phenyl azide to the 3x-TS (top row) and 3n-TS (bottom row) faces of norbornene.  $\Delta G^\ddagger$  values (kcal/mol) are shown below the Newman projections.

both termini of phenyl azide. The Newman projections for the endo cycloaddition of phenyl azide to norbornene show that the partially formed C–N bonds and the vicinal HCCH bonds suffer some eclipsing, while the  $\text{HCC}_{\text{bridged}}\text{H}$  eclipsing is severe, a factor noted originally by Schleyer for norbornyl solvolysis.<sup>25</sup>

The distortion/interaction model<sup>26</sup> is an approach to dissect activation barriers ( $\Delta E^\ddagger$ ) into distortion energy ( $\Delta E_{\text{d}}^\ddagger$ ) and interaction energy ( $\Delta E_{\text{i}}^\ddagger$ ). Distortion energy is the amount of energy required to bend phenyl azide and the dipolarophile into the transition-state geometry without allowing interaction. The interaction energy results from closed-shell (steric) repulsion, charge transfer from occupied-vacant orbital interactions, electron transfer, and polarization effects. The distortion/interaction model was used to analyze the reactivities and exostereoselectivities of these 1,3-dipolar cycloadditions. Since the dipolarophile is “pre-distorted” into the geometry of the exo transition state, the distortion energy is smaller for the exo transition states. This control of reactivity by distortion energies has been used to understand and design catalysts for palladium-catalyzed allylic alkylations.<sup>27</sup> Bickelhaupt has developed the activation strain model<sup>28</sup> to explain  $\text{S}_{\text{N}}2$  reactions and the enhanced reactivity of predistorted catalytically active transition-metal complexes.<sup>29</sup> Our group describes this as the distortion/interaction model and been applied to Diels–Alder reactions and 1,3-dipolar cycloadditions.<sup>30,31,35</sup>

We first established that computed activation free energies correspond reasonably well to experimental values, when available. Table 1 shows a comparison of the experimental activation barriers to the computed barriers using M06-2X/6-311G(d,p) and SCS-MP2/6-311G(d,p)//M06-2X/6-311G(d,p). Table 1 shows that M06-2X predicts activation barriers better than SCS-MP2. Both predict higher activation barriers than  $\Delta G^\ddagger_{\text{expt}}$ . Both give the correct order of reactants, but M06-2X gives an experimentally good correlation.

Table 2 gives the computed activation barriers ( $\Delta G^\ddagger$ ,  $\Delta H^\ddagger$ ,  $\Delta E^\ddagger$ ) distortion and interaction energies, and the NNN angle in each transition structure studied here. There is a large range of activation energies,  $\Delta E^\ddagger$  (3–27 kcal/mol), and a similarly large range of distortion energies,  $\Delta E_{\text{d}}^\ddagger$  (12–38 kcal/mol), but a relatively small range of interaction energies,  $\Delta E_{\text{i}}^\ddagger$  (8–14 kcal/mol). The distortion energies of the alkenes control barrier heights (Table 1), while the interaction energies are nearly constant. The range of alkene distortion energies (2–23 kcal/mol) is notably larger than the range of distortion energies of phenyl azide (15–25 kcal/mol), although the latter are generally larger than the former. Figure 5 shows a plot of  $\Delta E^\ddagger$  vs  $\Delta E_{\text{d}}^\ddagger$  for the seven reactions studied. There is an excellent linear correlation between distortion energy and activation energy ( $r^2 = 0.96$ ). Similar relationships have been observed for the cycloadditions of many dipoles and dienes with simple alkenes<sup>34–36</sup> and for related reactions by Bickelhaupt and co-workers.<sup>37,38</sup> It was previously shown with 1,3-dipolar cycloadditions of acetylene and ethylene with many dipoles the distortion of the 1,3-dipole comprises  $\sim 80\%$  of the distortion energy.<sup>30</sup> This portion of the total distortion energy is referred to as dipole distortion energy in this work and is defined as the energy required to bend the dipole into its transition structure geometry from its equilibrium geometry. In the azide cycloaddition studied here with unstrained 1 and 2, dipole distortion energies comprise 75% of the total distortion energy. In the series of strained alkenes studied here, dipole distortion energy makes up 40–90% of the total distortion energy.

**Table 1.**  $\Delta G^\ddagger_{\text{expt}}$ <sup>a</sup> Values Derived from Experimental Rate Constants.  $\Delta G^\ddagger_{\text{comp}}$  Energies Include Solvation by CPCM (CCl<sub>4</sub> or Et<sub>2</sub>O). Reactions of Phenyl Azide with Dipolarophiles **2**, **3**, and **7** As Calculated by M06-2X/6-311G(d,p) and [SCS-MP2/6-311G(d,p)//M06-2X/6-311G(d,p)] (Linear Regression Shown Below<sup>c</sup>)

alkene	solvent	T (°C)	10 <sup>7</sup> k <sub>2</sub> (M <sup>-1</sup> s <sup>-1</sup> )	$\Delta G^\ddagger_{\text{expt}}$ <sup>a,b</sup> (kcal/mol)	$\Delta G^\ddagger_{\text{M06-2X}}$ (kcal/mol)	$\Delta G^\ddagger_{\text{SCS-MP2}}$ (kcal/mol)
cyclohexene <sup>32</sup>	CCl <sub>4</sub>	25	0.03	29.0	33.1	32.1
norbornene <sup>35</sup>	CCl <sub>4</sub>	25	188	23.9	28.2	29.0
<i>anti</i> -sesquinorbornene <sup>33</sup>	Et <sub>2</sub> O	30	270	23.6	27.4	25.3

<sup>a</sup>Calculated from  $k = 6 \times 10^{12} e^{(-\Delta G^\ddagger/RT)}$ , derived as shown in the Supporting Information. <sup>b</sup>Computed free energies in solution are for the standard state of 1 M. <sup>c</sup>Linear regression between  $\Delta G^\ddagger_{\text{calc}}$  and  $\Delta G^\ddagger_{\text{expt}}$  for M06-2X and SCS-MP2 methods. M06-2X/6-311G(d,p)  $\Delta G^\ddagger_{\text{calc}} = 1.01\Delta G^\ddagger_{\text{expt}} + 3.72$ ;  $R^2 = 0.99$  and SCS-MP2/6-311G(d,p)//M06-2X/6-311G(d,p)  $\Delta G^\ddagger_{\text{calc}} = 0.97\Delta G^\ddagger_{\text{expt}} + 4.05$ ;  $R^2 = 0.75$ .

**Table 2.** M06-2X/6-311G(d,p) Activation Free Energies and Enthalpies of Activation, Electronic Energies of Activation, Distortion Energies, and Interaction Energies for the Reactions of Phenyl Azide and Dipolarophiles **1–7** (x = exo, n = endo;  $\angle\text{NNN}$  Is the Azide Bond Angle in Each Respective Transition Structure)

alkene	$\Delta G^\ddagger$	$\Delta H^\ddagger$	$\Delta E^\ddagger$	$\Delta H_{\text{cm}}$	$\Delta E_{\text{d}}^\ddagger$ alkene	$\Delta E_{\text{d}}^\ddagger$ PhN <sub>3</sub>	$\Delta E_{\text{d}}^\ddagger$ total	$\Delta E_{\text{i}}^\ddagger$	$\angle\text{NNN}$ (deg)
<b>1</b>	32.8	19.6	19.1	-29.2	7.6	23.4	31.1	12.0	137.3
<b>2</b>	32.2	19.6	19.2	-26.8	8.2	25.1	33.3	14.1	135.6
<b>3x</b>	27.5	14.7	14.4	-38.1	4.6	20.5	25.0	10.7	139.4
<b>3n</b>	34.9	21.7	21.1	-36.5	10.8	21.1	31.9	10.8	138.7
<b>4x</b>	16.0	3.3	3.1	-68.6	0.9	10.6	11.5	8.4	150.3
<b>4n</b>	21.6	9.3	9.0	-71.9	9.0	8.2	17.2	8.2	153.3
<b>5x</b>	22.1	8.7	8.3	-51.0	2.5	16.4	18.9	10.6	143.6
<b>5n</b>	30.8	17.6	17.2	-53.7	12.6	15.1	27.7	10.5	143.9
<b>6x</b>	26.2	12.1	11.7	-33.4	3.9	21.2	25.1	13.4	138.8
<b>6n</b>	40.3	27.1	27.2	-41.3	22.6	15.7	38.3	11.1	143.0
<b>7</b>	26.4	13.8	17.6	-46.5	6.7	17.7	29.0	11.4	141.1

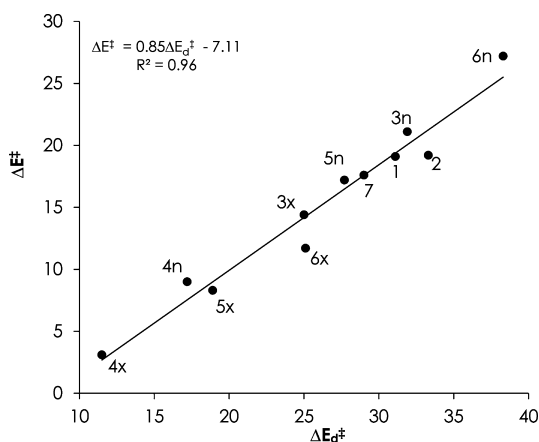


**Figure 5.** Plot of activation energies and distortion energies of the reactions of phenyl azide and dipolarophiles **1–7** calculated by M06-2X/6-311G(d,p). Values in kcal/mol.

Despite the rather remarkable fit in Figure 3, two outliers, **6x** and **6n** are apparent.

The activation barriers for the 1,3-dipolar cycloaddition of *syn*-sesquinorbornene deviate because of severe steric clashes in the endo transition structures (Figure 3). This effect appears in the distortion energy as well.

Pyramidalization plays a key role in the reactivity and stereoselectivity of these strained cycloalkenes undergoing 1,3-dipolar cycloadditions. The extent of pyramidalization ( $\theta_{\text{dih}}$ ) of the disubstituted alkenes (**1–5**) is first described, followed by the tetrasubstituted alkenes (**6–7**). Norbornene (**3**) is the least pyramidalized alkene ( $\theta_{\text{dih}} = 8^\circ$ ), and the  $\Delta E^\ddagger$  of **3x**-TS is 14 kcal/mol, the highest among pyramidalized alkenes. The distortion energy of phenyl azide is similar for both transition states, but the large difference between alkene distortion

energies favors the exo transition state (4.6 vs 10.8 kcal/mol). The  $\theta_{\text{dih}}$  of **5** is  $21^\circ$ , and the  $\Delta E^\ddagger$  drops to 8.3 kcal/mol. The lowered activation barrier is due to reduced distortion energy of the alkene and phenyl azide. The reduced distortion energy of phenyl azide results from the earlier transition state involving the distorted alkene. The largest  $\theta_{\text{dih}}$  is seen in the optimized structure of **4**, and the smallest  $\Delta E_{\text{d}}^\ddagger$  and  $\Delta E^\ddagger$  occur with **4x**-TS (11.5 and 3.1 kcal/mol, respectively). A remarkably small 0.9 kcal/mol is required to distort **4** into the exo transition state geometry, and 10.6 kcal/mol is required to distort phenyl azide into the NNN of  $150^\circ$  in the transition structure.

*syn*-Sesquinorbornene (**6**) has  $\theta_{\text{dih}} = 16.8^\circ$ ; the distortion energies for **6x**-TS is 3.9 kcal/mol and for **6n**-TS is 22.6 kcal/mol. The steric clashes of the hydrogens at carbons 3, 4, 8, and 9 with the azide contribute to the large difference in distortion energy,  $\Delta\Delta E_{\text{d}}^\ddagger$  (13.2 kcal/mol). *anti*-Sesquinorbornene is planar like *cis*-2-butene and cyclohexene, but the transition state shows a greater  $\angle\text{NNN}$  than that of **1**-TS and **2**-TS. As a result, the dipole distortion energy is 6 kcal/mol lower than that of **1**-TS. The relatively early transition state requires less bending of phenyl azide, which results in a lower activation barrier. The  $\Delta E^\ddagger$  for the reaction of tetramethylethylene with phenyl azide is 5.3 kcal/mol higher than for the reaction of antisquinorbornene with phenyl azide (see the Supporting Information). The strained nature of the *anti*-sesquinorbornene compared to tetramethylethylene results in the lower distortion energy.

Figure 6 correlates pyramidalization ( $\theta_{\text{dih}}$ ) to reactivity ( $\Delta H^\ddagger$ ) for the stereochemically preferred reactions of **1–6** with phenyl azide. The planar alkenes, **1** and **2** have nearly identical activation enthalpies. It is apparent that even slight pyramidalization of alkenes can greatly accelerate 1,3-dipolar cycloadditions. When  $\theta_{\text{dih}} = 4^\circ$ ,  $\Delta H^\ddagger$  is lowered by 1.4 kcal/mol, which corresponds to an order of magnitude acceleration



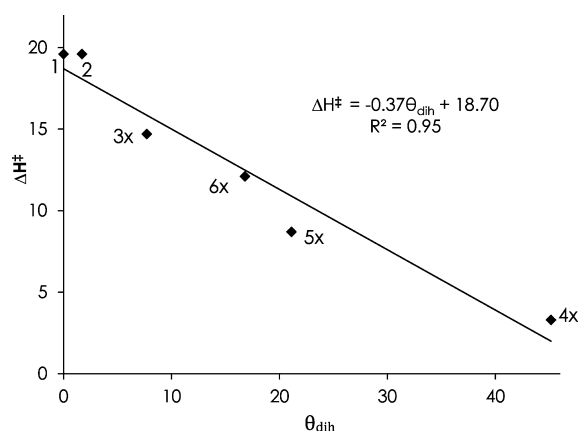


**Figure 6.** Plot of activation enthalpy (kcal/mol) vs  $\theta_{\text{dih}}$  (deg), calculated with M06-2X/6-311G(d,p).

at 25 °C.  $\Delta H^\ddagger$  is 0 kcal/mol when the  $\theta_{\text{dih}} = 51^\circ$ . For comparison, perfectly pyramidal  $\text{sp}^3$  carbon has a corresponding  $\theta_{\text{dih}}$  of  $60^\circ$ . It is notable that endo attack is also accelerated in the cases of high pyramidalization, compared to the unstrained alkenes. The degree of bending is an indication of the ease of out-of-plane bending and the magnitude of distortion energies.

The role of strain release in controlling reactivity was investigated by comparing  $\Delta H^\ddagger$  vs  $\Delta H_{\text{rxn}}$  in Figure 7. The energies of reaction used in this plot are shown in Table 1.

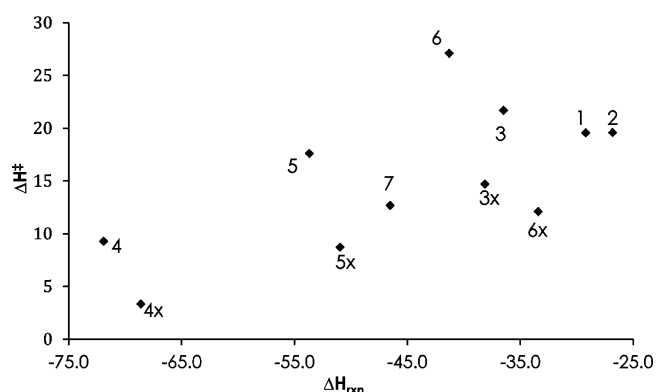


**Figure 7.** Plot of  $\Delta H^\ddagger$  vs  $\Delta H_{\text{rxn}}$ , calculated by M06-2X/6-311G(d,p).  $\Delta H^\ddagger = 0.30\Delta H_{\text{rxn}} + 28.61$ ;  $R^2 = 0.43$ .

There is no significant correlation of these quantities and  $R^2 = 0.43$ . Consequently, there is no clear Dimroth, Brønsted, Evans–Polanyi, or Marcus relationship,<sup>39–41</sup> where the differences between activation barriers are about one-half of the differences in energies of reaction. Strain release, as measured by the change of energy upon reaction, shows only a qualitative relationship to reaction rates. In Figure 7, the most strain is released with the substrates on the left side of the graph, but only 4x shows unusually high reactivity. The lack of relationship between activation barrier and strain release indicates that the enhanced reactivities of these strained alkenes are not “strain-promoted”. We have shown instead that they are distortion-accelerated when the ease of distortion to the transition-state geometry is lowered.

## CONCLUSION

The computations reported for a series of highly strained alkenes demonstrate the powerful effect that distortion and

pyramidalization have on 1,3-dipolar cycloadditions of alkenes. Pyramidalization is a form of predistortion that causes the alkene to geometrically resemble the exo transition structure. Less distortion energy is required to achieve this transition state, and the activation energy is correspondingly lessened. Alkenes with planar double bonds such as *cis*-2-butene and cyclohexene have much higher barriers, since the dipolarophiles and phenyl azide must undergo significant distortion to achieve the transition-state geometry. A strained cycloalkene with a pyramidalization of just  $4^\circ$  accelerates the reaction by an order of magnitude. While reactions of this type are often called strain-promoted, this study and others by our group<sup>42–44</sup> indicate that reduction of distortion energy controls rates of cycloaddition. This can be manifested in predistortion as in 3–6 discussed here or in reduction of distortion energies caused by angle strain as in cyclopropene.<sup>45–47</sup> The reactions are distortion-accelerated, subtly different from strain-promoted. The strain results in a predistortion of the alkene, which resembles the transition structure. Reduced distortion energy results in distortion-accelerated reactions.

## ASSOCIATED CONTENT

### Supporting Information

Calculated geometries and energies with M06-2X and SCS-MP2 methods; solvation energies; complete reference for Gaussian 09. This information is available free of charge via the Internet at <http://pubs.acs.org>.

## AUTHOR INFORMATION

### Corresponding Author

\*E-mail: [houk@chem.ucla.edu](mailto:houk@chem.ucla.edu).

### Notes

The authors declare no competing financial interest.

## ACKNOWLEDGMENTS

We thank the National Science Foundation (NSF CHE-1059084) for financial support of this research. The computations were performed on the UCLA IDRE Hoffman2 cluster.

## REFERENCES

- Vazquez, S.; Camps, P. *Tetrahedron* **2005**, *61*, 5147–5208.
- Sletten, E. M.; Bertozzi, C. R. *Acc. Chem. Res.* **2011**, *44*, 666.
- Han, H.-S.; Devaraj, N. K.; Lee, J.; Hilderbrand, S. A.; Weissleder, R.; Bawendi, M. G. *J. Am. Chem. Soc.* **2010**, *132*, 7838.
- Huisgen, R.; Moebius, L.; Mueller, G.; Stangl, H.; Szeimies, G.; Vernon, J. M. *Chem. Ber.* **1965**, *98*, 3992.
- Gutsmiedl, K.; Wirges, C. T.; Ehmke, V.; Carell, T. *Org. Lett.* **2009**, *11*, 2405.
- Hansell, C. F.; Espeel, P.; Stamenovic, M. M.; Barker, I. A.; Dove, A. P.; Du Prez, F. E.; O'Reilly, R. K. *J. Am. Chem. Soc.* **2011**, *133*, 13828.
- Watson, W. H.; Galloy, J.; Bartlett, P. D.; Roof, A. A. M. *J. Am. Chem. Soc.* **1981**, *103*, 2022.
- Huisgen, R.; Ooms, P. H. J.; Mingin, M.; Allinger, N. L. *J. Am. Chem. Soc.* **1980**, *102*, 3951.
- Rondan, N. G.; Paddon-Row, M. N.; Caramella, P.; Mareda, J.; Mueller, P. H.; Houk, K. N. *J. Am. Chem. Soc.* **1982**, *104*, 4974.
- Kolb, H. C.; Finn, M. G.; Sharpless, K. B. *Angew. Chem., Int. Ed.* **2001**, *40*, 2004.
- Frisch, M. J. et al. ( see complete reference in the Supporting Information ). *Gaussian 09*, revision A.1; Gaussian Inc.: Wallingford, CT, 2009.
- Zhao, Y.; Truhlar, D. G. *Theor. Chem. Acc.* **2008**, *120*, 215.

- (13) (a) Grimme, S. J. *J. Chem. Phys.* **2003**, *109*, 3067. (b) Grimme, S. J. *J. Chem. Phys.* **2003**, *118*, 9095. (c) Greenkamp, M.; Grimme, S. *Chem. Phys. Lett.* **2004**, *392*, 229.
- (14) Takano, Y.; Houk, K. N. *J. Chem. Theor. Comput.* **2005**, *1*, 70.
- (15) (a) Klamt, A.; Schüürmann, G. *J. Chem. Soc., Perkin Trans. 2* **1993**, 799. (b) Andzelm, J.; Kolmel, C.; Klamt, A. *J. Chem. Phys.* **1995**, *103*, 9312. (c) Barone, V.; Cossi, M. *J. Phys. Chem. A* **1998**, *102*, 1995. (d) Cossi, M.; Rega, N.; Scalmani, G.; Barone, V. *J. Comput. Chem.* **2003**, *24*, 669.
- (16) Zhao, Y.; Truhlar, D. G. *Phys. Chem. Chem. Phys.* **2008**, *10*, 2813.
- (17) Ribeiro, R. F.; Marenich, A. V.; Cramer, C. J.; Truhlar, D. G. *J. Phys. Chem. B* **2011**, *115*, 14556.
- (18) Lan, Y.; Zou, L.; Cao, Y.; Houk, K. N. *J. Phys. Chem. A* **2011**, *115*, 13906.
- (19) Houk, K. N.; Rondan, N. G.; Brown, F. K.; Jorgensen, W. L.; Madura, J. D.; Spellmeyer, D. C. *J. Am. Chem. Soc.* **1983**, *105*, 5980.
- (20) Williams, R. V.; Colvin, M. E.; Tran, N.; Warrenner, R. N.; Margetić, D. *J. Org. Chem.* **2000**, *65*, 562.
- (21) Holthausen, M. C.; Koch, W. *J. Phys. Chem.* **1993**, *97*, 10021.
- (22) Volland, W. V.; Davidson, E. R.; Borden, W. T. *J. Am. Chem. Soc.* **1979**, *101*, 533.
- (23) Williams, R. V.; Margetić, D. *J. Org. Chem.* **2004**, *69*, 7134.
- (24) Fernandez, J. A.; Vazquez, S. *Eur. J. Org. Chem.* **2007**, *27*, 4493.
- (25) Schleyer, P.; von, R. *J. Am. Chem. Soc.* **1964**, *86*, 1854.
- (26) Ess, D. H.; Houk, K. N. *J. Am. Chem. Soc.* **2007**, *129*, 10646.
- (27) Wassenaar, J.; Jansen, E.; Zeist, W.-J. v.; Bickelhaupt, F. M.; Siegler, M. A.; Spek, A. L.; Reek, J. N. H. *Nature Chem.* **2010**, *2*, 417.
- (28) de Jong, G. T.; Bickelhaupt, F. M. *ChemPhysChem* **2007**, *8*, 1170.
- (29) Zeist, W.-J. v.; Visser, R.; Bickelhaupt, F. M. *Chem. Eur. J.* **2009**, *15*, 6112.
- (30) Gordon, C.; Mackey, J. L.; Jewett, J. C.; Sletter, E. M.; Houk, K. N.; Bertozzi, C. R. *J. Am. Chem. Soc.* **2012**, *134*, 9199.
- (31) Ess, D. H.; Jones, G. O.; Houk, K. N. *Org. Lett.* **2008**, *10*, 1633.
- (32) Huisgen, R.; Moebius, L.; Mueller, G.; Stangl, H.; Szeimies, G.; Vernon, J. M. *Chem. Ber.* **1965**, *98*, 3992.
- (33) Watson, W. H.; Galloy, J.; Bartlett, P. D.; Roof, A. A. M. *J. Org. Chem.* **1985**, *50*, 4093.
- (34) Ess, D. H.; Houk, K. N. *J. Am. Chem. Soc.* **2008**, *130*, 10187.
- (35) Jones, G. O.; Houk, K. N. *J. Org. Chem.* **2008**, *73*, 1333.
- (36) Paton, R. S.; Kim, S.; Ross, A. G.; Danishefsky, S. J.; Houk, K. N. *Angew. Chem., Int. Ed.* **2011**, *50*, 10366.
- (37) Fernandez, I.; Cossio, F. P.; Bickelhaupt, F.; Matthias. *J. Org. Chem.* **2011**, *76*, 2310.
- (38) Fernandez, I.; Bickelhaupt, F.; Matthias. *J. Comput. Chem.* **2012**, *33*, 509.
- (39) Dimroth, O. *Angew. Chem.* **1933**, *46*, 571.
- (40) Evans, M. G.; Polanyi, M. *Trans. Faraday Soc.* **1936**, *32*, 1340.
- (41) Marcus, R. A. *J. Chem. Phys.* **1956**, *24*, 966.
- (42) Hayden, A.; Houk, K. N. *J. Am. Chem. Soc.* **2009**, *131*, 4084.
- (43) Osuna, S.; Houk, K. N. *Chem.—Eur. J.* **2009**, *15*, 13219.
- (44) Cheong, P. H.-Y.; Paton, R. S.; Bronner, S.; Im, G.-Yoon, J.; Garg, N. K.; Houk, K. N. *J. Am. Chem. Soc.* **2010**, *132*, 126.
- (45) Yang, J.; Seckute, J.; Cole, C. M.; Devaraj, N. K. *Angew. Chem., Int. Ed.* **2012**, DOI: 10.1002/anie.201202122.
- (46) Thalhammer, F.; Wallfahrer, U.; Sauer, J. *Tetrahedron Lett.* **1990**, *31*, 3851.
- (47) Sauer, J.; Bäuerlein, P.; Ebenbeck, W.; Gousetis, C.; Sichert, H.; Troll, T.; Utz, F.; Wallfahrer, U. *Eur. J. Org. Chem.* **2001**, 2629.